

# Carbodiimide-driven toughening of interpenetrated polymer networks

Chamoni W. H. Rajawasam,<sup>a</sup> Corvo Tran,<sup>a</sup> Jessica L. Sparks,<sup>b</sup> William H. Krueger,<sup>a</sup> C. Scott Hartley,<sup>a,\*</sup> and Dominik Konkolewicz<sup>a,\*</sup>

- a. Department of Chemistry and Biochemistry, Miami University, Oxford, OH, USA.
- b. Department of Chemical Paper and Biomedical Engineering, Miami University, Oxford, OH, USA.

## Abstract

Recent work has demonstrated that temporary crosslinks in polymer networks generated by chemical “fuels” afford materials with large, transient changes in their mechanical properties. This can be accomplished in carboxylic-acid-functionalized polymer hydrogels using carbodiimides, which generate anhydrides with lifetimes on the order of minutes to hours. Here, the impact of the polymer architecture on the mechanical properties of materials was explored. Single networks (SNs) were compared to interpenetrated networks (IPNs). Notably, semi-IPN precursors that give IPNs on treatment with the carbodiimide gave much higher fracture energies (i.e., resistance to fracture) and superior resistance to compressive strain compared to other network structures. A precursor semi-IPN material featuring acrylic acid in only the free polymer chains yields, on treatment with carbodiimide, an IPN with a fracture energy of 2400 J/m<sup>2</sup>, a fourfold increase compared to an analogous semi-IPN precursor that yields a SN. This resistance to fracture enables the formation of macroscopic complex cut patterns, even at high strain, underscoring the pivotal role of polymer architecture in mechanical performance.

## Introduction

Systems driven out of equilibrium by coupled chemical reactions have received significant attention recently because of their time-dependent properties.<sup>1,2</sup> They are analogous to many biological systems that operate using chemical “fuels”, such as ATP. Chemically driven processes can enhance a biomaterial’s mechanical properties or effect actuation. For example, muscle contraction happens as a result of the hydrolysis of ATP.<sup>3,4</sup> Drawing inspiration from nature, recent research has focused on leveraging chemical fuels to enhance mechanical properties of polymer materials,<sup>5–8</sup> and to drive controlled swelling<sup>9</sup> and phase separation.<sup>10</sup> These systems give transient changes in properties and are related to stimuli-responsive polymer hydrogels, which change their physical or chemical properties in response to, for example, light,<sup>11,12</sup> temperature,<sup>13</sup> pH<sup>14,15</sup> or electrical fields,<sup>16</sup> with potential applications in drug delivery,<sup>17,18</sup> as sensors,<sup>19,20</sup> and as wearable devices.<sup>21,22</sup>

Fueled systems change their properties over time driven by coupled reactions that are out of equilibrium, returning to their original “resting” states spontaneously.<sup>23</sup> The behavior of several fuel-mediated polymer hydrogels has recently been reported. Notably, Eelkema and co-workers<sup>24</sup> have demonstrated temporary hydrogel swelling driven by the decomposition of allylic acetates. The overall reaction is catalyzed by pyridine-containing hydrogels, which form (charged) quaternized intermediates. As the concentration of charges within the network increases, the

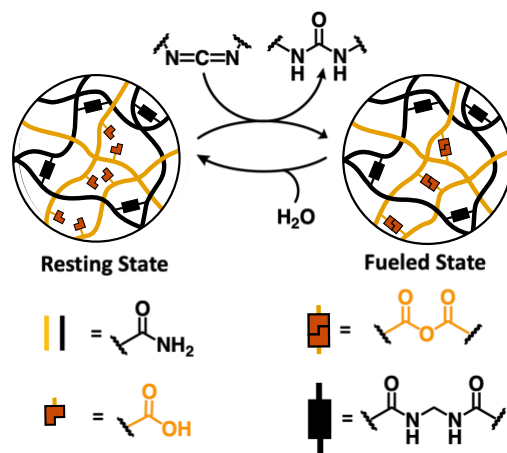
hydrogel swells because of an increase in osmotic pressure and repulsive forces between the charged groups. Similarly, Wang and co-workers<sup>25</sup> have developed a bilayer hydrogel actuator using urease to slowly basify an acidic solution that quaternizes an amine-functionalized hydrogel. Further, Wang and coworkers have developed hydrogels with shear thinning and self-healing properties based on temporary borate ester crosslinks.<sup>26</sup>

The coupling of carboxylic acids to anhydrides driven by carbodiimides,<sup>27,28</sup> usually 1-ethyl-3-(3-dimethylaminopropyl)carbodiimide (EDC), can be used to change polymer material properties through the modulation of the hydrophilicity of poly(acrylic acid) chains. This approach has been used by Walther co-workers to generate volume phase transitions in microgels,<sup>29</sup> and by Wang, Xuan, and co-workers in hydrogel actuators.<sup>9</sup> Our group has used EDC to control the crosslink density of polymer network hydrogels. The coupling of pendant acrylic acid groups in otherwise permanently crosslinked networks leads to the formation of temporary anhydride bonds, significantly enhancing the network strength and enabling temporally controlled adhesion and reversible patterning of mechanical properties.<sup>5</sup>

Polymer network architecture is a core feature of materials that describes the arrangement of the monomers along the backbone and the three-dimensional structure of the macromolecules.<sup>30</sup> It plays a crucial role in determining mechanical properties. Here, we investigate how the transient mechanical properties of fuel-responsive hydrogels change with network architecture. We compare various interpenetrating networks (IPNs) with single networks (SNs). IPN hydrogels have two or more polymer networks that are intertwined but not covalently bonded to each other.<sup>31</sup> This is distinct from SN materials where all linkers are on the same network backbone. Compared to SN hydrogels, IPN hydrogels have been shown to enhanced network strength, both intrinsically and in response to stimuli.<sup>32</sup>

An example of the chemical reaction network is shown in Scheme 1. Transient crosslinking was achieved by introducing acrylic acid into the backbone, which forms anhydrides in the presence of EDC (activation) that subsequently undergo hydrolysis (deactivation). After activation, these polymer systems therefore contain both transient (anhydride) and permanent (amide) crosslinkers. In the example in Scheme 1, the chemistry transforms a semi-interpenetrating network (semi-IPN), consisting of free polymer chains dispersed through a permanently crosslinked network without any interaction between two polymer systems, into a fully interpenetrating network. By comparing this system to other network architectures, we show that a material's architecture, before and after treatment with the fuel, has a substantial effect on its properties.

The four distinct classes of polymer materials presented in Table 1 were considered. Judicious choice of polymer network can give high performance materials on fueling, with unusual tolerance to fracture, thereby introducing a promising avenue for applications involving substantial mechanical challenges.

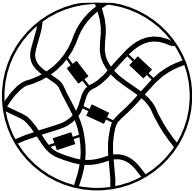
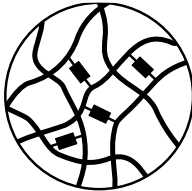



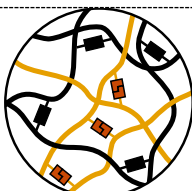




Scheme 1: Overview of chemically fueled anhydride formation.

## Results and Discussion

All materials incorporated acrylamide (Am) as a backbone-forming monomer that does not react with EDC, with *N,N'*-methylenebisacrylamide (MBAm) as a similar inert permanent crosslinker. The polymers were synthesized by reversible addition-fragmentation chain transfer (RAFT) polymerization using acrylic acid (AA) and Am as monomers, 2-(((ethylthio)carbonothioyl)thio) propionic acid (PAETC) and modified PAETC with PEG as the chain-transfer agents (CTA), and 2,2'-azobis[2-(2-imidazolin-2-yl)propane]dihydrochloride (VA-044) as the radical initiator. When synthesizing semi-IPN hydrogels, the free polymer served as the polymerization medium for the permanently crosslinked polymer. To ensure that the free polymer does not react during the formation of the second network, the RAFT end group was removed by aminolysis followed by Michael addition.<sup>33</sup> The semi-IPNs described in this study were synthesized using a 1:1 ratio of a free polymer, poly(Am<sub>X</sub>-AA<sub>Y</sub>), referred to as the first polymer, and a crosslinked polymer, poly(Am<sub>X</sub>-AA<sub>Y</sub>-MBAm<sub>1.3</sub>), referred to as the second polymer. The choice of 1.3 MBAm units was based on prior studies, which showed that 1.3 permanent crosslinkers per chain led to the highest change in mechanical properties upon addition of chemical fuel in Am/AA hydrogels where we could obtain a perfect solid material.<sup>5</sup> Two control materials were developed. A single network with no AA units, poly(Am<sub>X</sub>-MBAm<sub>1.3</sub>), was synthesized to highlight the significance of transient anhydride formation on addition of EDC, and a SN consisting of poly(Am<sub>X</sub>-AA<sub>Y</sub>-MBAm<sub>1.3</sub>) was prepared to highlight the impact of polymer network architecture.

Table 1: Different polymer architectures before and after treatment with EDC.

Architecture	Before adding EDC	After adding EDC
a) poly(Am <sub>X</sub> -MBAm <sub>1.3</sub> )	 SN	 SN
b) poly(Am <sub>X</sub> -AA <sub>Y</sub> -MBAm <sub>1.3</sub> )	 SN	 SN
c) poly(Am <sub>X</sub> -AA <sub>Y</sub> )/ (Am <sub>X</sub> -MBAm <sub>1.3</sub> )	 semi-IPN	 IPN
d) poly(Am <sub>X</sub> -AA <sub>Y</sub> )/ (Am <sub>X</sub> -AA <sub>Y</sub> -MBAm <sub>1.3</sub> )	 semi-IPN	 SN

Initial studies focused on the effect of EDC on the rheological properties of hydrogels poly(Am<sub>70</sub>-AA<sub>30</sub>)/(Am<sub>100</sub>-MBAm<sub>1.3</sub>) and poly(Am<sub>85</sub>-AA<sub>15</sub>)/(Am<sub>100</sub>-MBAm<sub>1.3</sub>), which are semi-IPNs with acid groups in only the first network, and thus should yield IPNs after fueling; poly(Am<sub>70</sub>-AA<sub>30</sub>)/(Am<sub>70</sub>-AA<sub>30</sub>-MBAm<sub>1.3</sub>), poly(Am<sub>85</sub>-AA<sub>15</sub>)/(Am<sub>70</sub>-AA<sub>30</sub>-MBAm<sub>1.3</sub>), and poly(Am<sub>70</sub>-AA<sub>30</sub>)/(Am<sub>85</sub>-AA<sub>15</sub>-MBAm<sub>1.3</sub>), which are semi-IPNs with acid groups in both networks, and should yield SNs; and controls poly(AA<sub>70</sub>-Am<sub>30</sub>-MBAm<sub>1.3</sub>) and poly(Am<sub>100</sub>-MBAm<sub>1.3</sub>). Solutions of EDC (2.00 M, 2.00 mL) were introduced above and below disc-shaped samples of each material, which were then monitored by rheological time sweep experiments. Both the storage ( $G'$ ) and loss ( $G''$ ) moduli increased and gradually returned to their initial values, as depicted in Figures 1 and S1-5, except in the case of the acid-free control poly(Am<sub>100</sub>-MBAm<sub>1.3</sub>) (Figure S1). This is consistent with the EDC producing transient anhydride crosslinks, converting the semi-IPN into a fully percolated SN or an IPN depending on the primary chain structure,

thereby altering its mechanical properties.<sup>34</sup> In all cases (other than the control), the storage moduli reach a maximum point ( $G'_{\max}$ ) at the maximum crosslinking density.

The three polymer systems in Figure 1, poly(Am70-AA30)/(Am100-MBAm1.3), poly(Am70-AA30)/(Am70-AA30-MBAm1.3), and poly(Am70-AA30-MBAm1.3), are useful representative examples. Poly(Am70-AA30)/(Am100-MBAm1.3) undergoes a transformation from a semi-IPN to a transient IPN, poly(Am70-AA30)/(Am70-AA30-MBAm1.3) changes from a semi-IPN to a transient SN, and poly(Am70-AA30-MBAm1.3) is an SN throughout (albeit with changing crosslink density). We expected that the IPN would exhibit a higher  $G'_{\max}$  compared to an SN.<sup>35</sup> However, the SN poly(Am70-AA30-MBAm1.3) reached a  $G'_{\max}$  of around 140 kPa (Figure 1c),<sup>5</sup> whereas the transient IPN with the same moles of acid groups in the first polymer, poly(Am70-AA30)/(Am100-MBAm1.3) reached a  $G'_{\max}$  of only 3 kPa. The poly(Am70-AA30)/(Am70-AA30-MBAm1.3) was in the middle, with a  $G'_{\max}$  22.

The absence of AA units in the permanent network of poly(Am100-MBAm1.3) likely reduces the total anhydride crosslink density. In contrast, the SN hydrogel, which contains AA units in its entire network, forms a more densely crosslinked structure, resulting a higher  $G'_{\max}$ . This discrepancy may also be due to the formation of clusters of high crosslink density upon EDC fueling in the systems that start from semi-IPN structures. This may not lead to a large increase in overall  $G'$  but could give pockets of anhydrides able to exchange and eventually hydrolyze. This hypothesis is further supported by the lower  $G'_{\max}$  for poly(Am70-AA30)/(Am70-AA30-MBAm1.3) when compared to SN poly(Am70-AA30-MBAm1.3). The  $G'_{\max}$  of poly(Am70-AA30)/(Am85-AA15-MBAm1.3) is lower than that of poly(Am85-AA15)/poly(Am70-AA30-MBAm1.3) (Figures S2, S3 and Table S2). This observation suggests that, in the IPN hydrogel, the presence of more AA in the crosslinked or the second network results in a higher accessibility of carboxylic acids for EDC coupling.

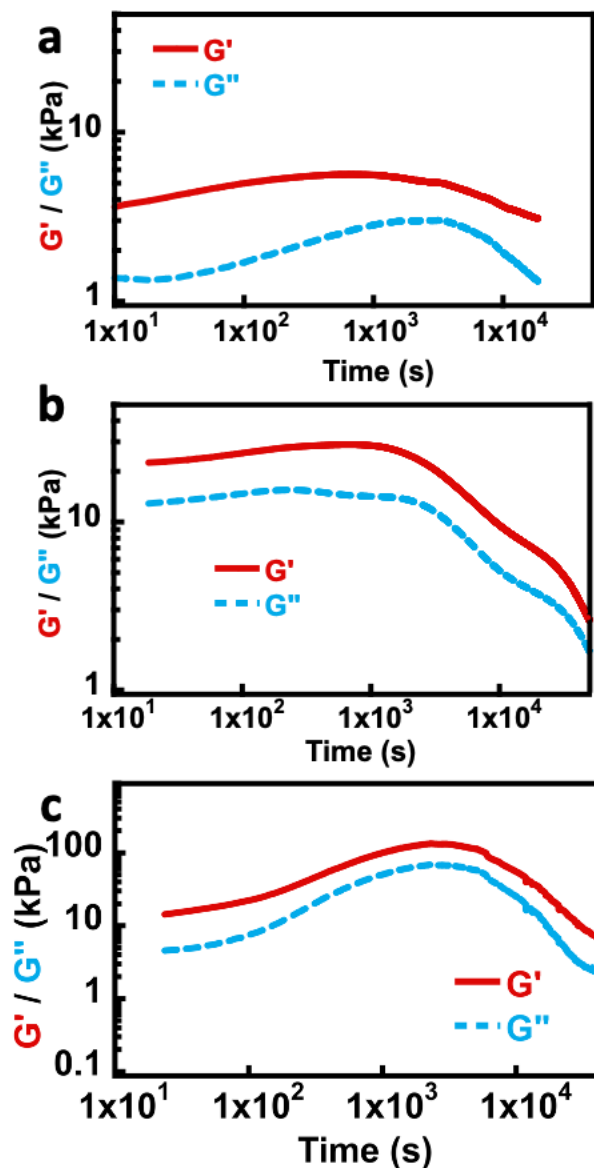


Figure 1: Rheological time sweeps of (a) poly(Am<sub>70</sub>-AA<sub>30</sub>)/(Am<sub>100</sub>-MBAm<sub>1.3</sub>), (b) poly(Am<sub>70</sub>-AA<sub>30</sub>)/(Am<sub>70</sub>-AA<sub>30</sub>-MBAm<sub>1.3</sub>) and (c) poly(Am<sub>70</sub>-AA<sub>30</sub>-MBAm<sub>1.3</sub>) after fueling with EDC at 4 °C

To evaluate the materials' behavior under uniaxial mechanical testing conditions, compressive stress strain curves, followed by stress-relaxation tests were conducted on three different materials: SN hydrogel poly(Am<sub>70</sub>-AA<sub>30</sub>-MBAm<sub>1.3</sub>) and the semi-IPN systems poly(Am<sub>70</sub>-AA<sub>30</sub>)/(Am<sub>100</sub>-MBAm<sub>1.3</sub>) and poly(Am<sub>70</sub>-AA<sub>30</sub>)/(Am<sub>70</sub>-AA<sub>30</sub>-MBAm<sub>1.3</sub>). The materials were tested in both the resting (semi-IPN vs SN) and transiently crosslinked states (IPN vs SN). The stress-strain results are shown in Figure 2 with stress relaxation shown in Figure S7. In the presence of EDC, all materials tolerate high compression stress because the formation of anhydride bonds increases their ability to resist deformation. The two IPN systems are compared in Figure 2a. In contrast to the rheology, where poly(Am<sub>70</sub>-AA<sub>30</sub>)/(Am<sub>70</sub>-AA<sub>30</sub>-MBAm<sub>1.3</sub>) showed the higher  $G'_{max}$ , poly(Am<sub>70</sub>-AA<sub>30</sub>)/(Am<sub>100</sub>-MBAm<sub>1.3</sub>) resisted higher compressive stress than poly(Am<sub>70</sub>-AA<sub>30</sub>)/(Am<sub>70</sub>-AA<sub>30</sub>-MBAm<sub>1.3</sub>) (Figures 2c and 2d). This may be because the poly(Am<sub>70</sub>-AA<sub>30</sub>)/(Am<sub>100</sub>-MBAm<sub>1.3</sub>) retains the entanglements in an IPN after fueling and has

effective rupture and reformation of anhydride bonds giving energy dissipation, with the second polymer (poly(Am<sub>100</sub>-MBAm<sub>1.3</sub>)) maintaining overall structure under significant deformation. For this reason, IPNs have the capability to resist higher compression in other reported systems.<sup>36</sup> This finding highlights the significant difference in materials' properties between the linear and nonlinear viscoelastic regimes. When treated with water alone (i.e., no EDC), the two semi-IPNs show two different compression stress curves. This suggests that different monomer compositions may also contribute to the variation in compression stress values.

In contrast to the IPNs, the single network poly(Am<sub>70</sub>-AA<sub>30</sub>-MBAm<sub>1.3</sub>) hydrogel broke under 60% compression, as seen in Figures 2b and 2e. Because of its higher anhydride crosslinking density, its compression stress is much higher than that of the IPNs. This trend of higher modulus for the poly(Am<sub>70</sub>-AA<sub>30</sub>-MBAm<sub>1.3</sub>) compared to the IPNs was also seen in the rheological time sweeps. Figures 2 and S7 show that the IPN poly(Am<sub>70</sub>-AA<sub>30</sub>)/poly(Am<sub>100</sub>-MBAm<sub>1.3</sub>) was able to relax more rapidly than the other compositions showing rapid decrease in stress after 60% compression, allowing it to regain its initial shape within a short period of time, presumably because of the uncrosslinked poly(Am<sub>100</sub>-MBAm<sub>1.3</sub>) network (without anhydride crosslinks) driving rearrangement back to the original structure. Additionally, as shown in Figure S8 after the consumption of all EDC and subsequent hydrolysis, the transient IPN poly(Am<sub>70</sub>-AA<sub>30</sub>)/(Am<sub>100</sub>-MBAm<sub>1.3</sub>) essentially returned to its resting semi-IPN state within 6 hours. The maximum compression stress at this point was similar to that of the control experiment where the polymer was treated with water instead of EDC. The material could then be refueled and regained the transient IPN's performance under compression.

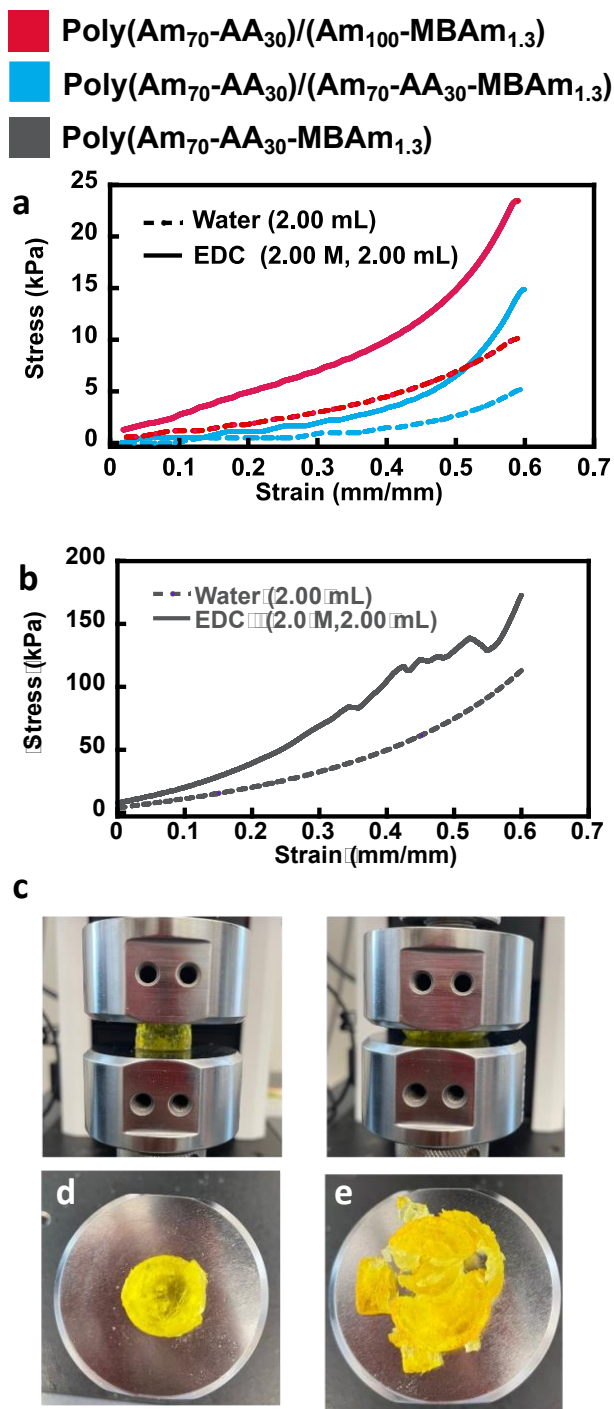


Figure 2: Compressive stress-strain results for (a) poly(Am<sub>70</sub>-AA<sub>30</sub>)/(Am<sub>100</sub>-MBAm<sub>1.3</sub>) and poly(Am<sub>70</sub>-AA<sub>30</sub>)/(Am<sub>70</sub>-AA<sub>30</sub>-MBAm<sub>1.3</sub>) and (b) poly(Am<sub>70</sub>-AA<sub>30</sub>-MBAm<sub>1.3</sub>). (c) Images of poly(Am<sub>70</sub>-AA<sub>30</sub>)/(Am<sub>100</sub>-MBAm<sub>1.3</sub>) before and at 60% compression in the presence EDC. (d) Image of poly(Am<sub>70</sub>-AA<sub>30</sub>)/(Am<sub>100</sub>-MBAm<sub>1.3</sub>) after 60% compression in the presence EDC. (e) Image of poly(Am<sub>70</sub>-AA<sub>30</sub>-MBAm<sub>1.3</sub>) after 60% compression in the presence EDC.

The impact of network architecture on the materials' fracture energies ( $\Gamma$ , the measure of a material's resistance to a fracture<sup>37</sup>) was evaluated in the presence and absence of EDC.  $\Gamma$  was calculated using stress-strain curves of paired notched and pristine samples (see Supporting Information), adapting the method outlined by Zhao.<sup>38,39</sup> When a gel with a notch is stretched, the



notch becomes a running crack that eventually leads to rupture of the polymer at a strain of  $\epsilon_{\text{notch}}$ . The fracture energy is calculated from a pristine sample as the area under the stress strain curve from a strain of 0 to  $\epsilon_{\text{notch}}$  using equation 1, where  $h$  is the unnotched sample's initial height and  $\sigma$  is the stress of the specific material.

$$\Gamma = h \int_0^{\epsilon_{\text{notch}}} \sigma d\epsilon \quad (1)$$

As shown in Figure 3, the fracture energies of all hydrogels containing AA were significantly higher in the presence of EDC than when treated with only water. The formation of anhydride crosslinks increases the strength and toughness of the material and may inhibit the propagation of the crack. There was no significant difference in fracture energy between adding EDC and adding water for the control, poly(Am<sub>100</sub>-MABm<sub>1.3</sub>). Figure 3 also shows that materials that started from the semi-IPNs have higher fracture energy values than the SN poly(Am<sub>70</sub>-AA<sub>30</sub>-MBAm<sub>1.3</sub>). This is true with and without EDC and can be attributed to the greater number of entanglements present in the IPNs, leading to an increase in cohesive forces.<sup>40</sup> Interestingly, this is preserved even when both networks contain AA, which form a single network after adding EDC, possibly because of the preservation of entanglements from the resting state.

Remarkably, poly(Am<sub>70</sub>-AA<sub>30</sub>)/(Am<sub>100</sub>-MBAm<sub>1.3</sub>), giving a transient IPN, showed the largest fracture energy on treatment with EDC, reaching 2400 J/m<sup>2</sup>, one order of magnitude higher than when only water was added and four times greater than the materials that contained acid groups in both networks. This result is in sharp contrast to the rheological time sweep data, where the transient IPN materials exhibited the lowest  $G'_{\text{max}}$ . This behavior suggests that poly(Am<sub>70</sub>-AA<sub>30</sub>)/(Am<sub>100</sub>-MBAm<sub>1.3</sub>) behaves as a truly independent double-network gel in the fueled state, with no covalent interconnection between the two polymer networks. This transient material is a loosely packed structure of the permanent poly(Am<sub>100</sub>-MBAm<sub>1.3</sub>) network with clustered anhydride-crosslinked poly(Am<sub>70</sub>-AA<sub>30</sub>) chains entwined around it. When strained, energy dissipation can occur by anhydride bond exchange,<sup>41</sup> allowing for recovery.<sup>42</sup> The other transient IPN, poly(Am<sub>85</sub>-AA<sub>15</sub>)/(Am<sub>100</sub>-MBAm<sub>1.3</sub>), shows the second-highest fracture energy of 1400 J/m<sup>2</sup> despite having the lowest proportion of acid groups of all materials studied (excluding the poly(Am) only control).

The transient SNs derived from semi-IPN with AA in both polymer networks exhibit lower fracture energies than the two transient IPNs. This difference underlines the importance of network architecture in determining transient properties. For the same architecture, systems with higher proportions of AA have higher fracture energies in the fueled states.

The high fracture energy of 2400 J/m<sup>2</sup> for poly(Am<sub>70</sub>-AA<sub>30</sub>)/(Am<sub>100</sub>-MBAm<sub>1.3</sub>) compares well with those of reported high-performing polymer networks. For example, composite hydrogels incorporating layer inorganic micro sized platelets from Kim and coworkers<sup>43</sup> achieve a fracture energy of around 2000 J/m<sup>2</sup>. Mooney and co-workers presented a hydrogel combining ionic and covalent networks which led to higher fracture energies surpassing 6000 J/m<sup>2</sup>.<sup>44</sup> The materials discussed here provide temporary high fracture energies on demand while maintaining flexibility and lower modulus in the resting state.

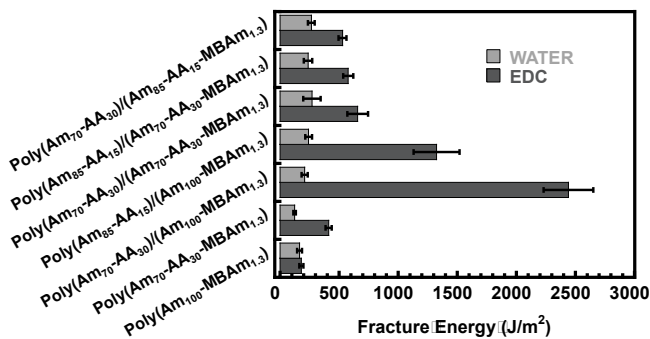


Figure 3: Fracture energies of different polymer architecture

To confirm that the increases in fracture energy are caused by the EDC-generated anhydride bonds that can be regenerated, the poly(Am<sub>70</sub>-AA<sub>30</sub>)/(Am<sub>100</sub>-MBAm<sub>1.3</sub>) and poly(Am<sub>70</sub>-AA<sub>30</sub>-MBAm<sub>1.3</sub>) systems were subjected to repeated EDC treatments. As shown in Figure 4, after an initial treatment with EDC that increases the fracture energies, both the poly(Am<sub>70</sub>-AA<sub>30</sub>-MBAm<sub>1.3</sub>) and poly(Am<sub>70</sub>-AA<sub>30</sub>)/(Am<sub>100</sub>-MBAm<sub>1.3</sub>) hydrogels returned to their resting states after 6 hours, consistent with complete anhydride bonds hydrolysis. When subjected to another treatment with EDC, the materials achieve fracture energies similar to the first fueling cycle showing no significant change in fracture energy.

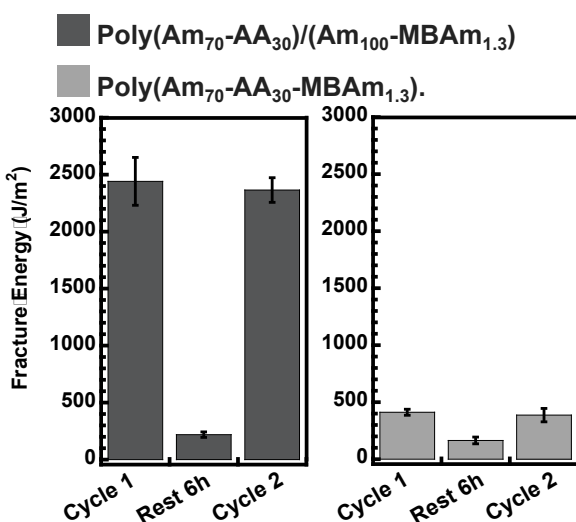


Figure 4: Evolution of fracture energy of different polymer architectures.

The higher fracture resistance observed for the poly(Am<sub>70</sub>-AA<sub>30</sub>)/(Am<sub>100</sub>-MBAm<sub>1.3</sub>) enabled exploration of the performance of these materials under mechanically challenging conditions. Figures 5a and 5b show the resistance of SN poly(Am<sub>70</sub>-AA<sub>30</sub>-mBAm<sub>1.3</sub>) and the transient IPN poly(Am<sub>70</sub>-AA<sub>30</sub>)/(Am<sub>100</sub>-MBAm<sub>1.3</sub>) to a single hole punched in their centers. In both cases, the EDC-fueled state was capable of reaching higher strain before failure compared to materials treated with only water. The difference for poly(Am<sub>70</sub>-AA<sub>30</sub>-mBAm<sub>1.3</sub>) is fairly small of around 0.10 mm/mm, as shown in Figure 5a. Notably, however, the transient IPN from poly(Am<sub>70</sub>-AA<sub>30</sub>)/(Am<sub>100</sub>-MBAm<sub>1.3</sub>) exhibited a significant tolerance compared to SN as illustrated in Figure 5b, with a strain at break of nearly 5 compared to <1 for the SN materials or the same material without EDC. This indicates that the formation of anhydride bonds within the hydrogel over time

was able to maintain the material's bulk structure even under applied strain. It is possible that at higher strains, the anhydrides can exchange with free acids, enhancing energy and stress dissipation in the materials improving toughness and tolerance to fractures.<sup>45</sup> Including multiple cuts in the material yields kirigami-like patterns on stretching,<sup>46</sup> that is, designs that involve cutting and folding materials to create intricate shapes as in Figure 5c and d.

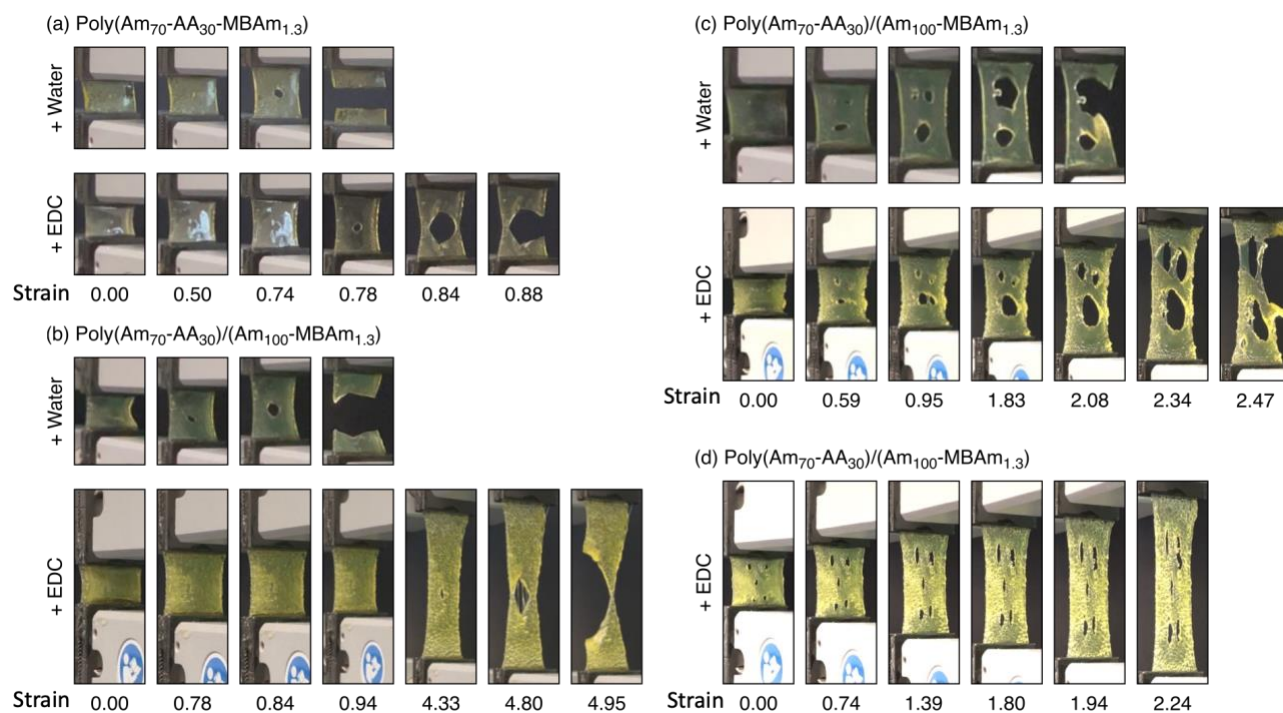


Figure 5: Images of strained materials with a hole cut out for (a) poly(Am<sub>70</sub>-AA<sub>30</sub>-MBAm<sub>1.3</sub>) and (b) poly(Am<sub>70</sub>-AA<sub>30</sub>)/poly(Am<sub>100</sub>-MBAm<sub>1.3</sub>). (c, d) Multiple-hole kirigami patterning of poly(Am<sub>70</sub>-AA<sub>30</sub>)/poly(Am<sub>100</sub>-MBAm<sub>1.3</sub>). Values on x axis represent applied strain.

Figures 6 and S7 illustrate how the polymer architecture affects an EDC-mediated polymer system. The results highlight that modulus is not predictive of fracture resistance. When EDC is present, polymers containing acid groups in both the first and second networks transform into a single network. This transformation leads to a higher maximum storage modulus ( $G'_{max}$ ), which is an indicator of stiffness. However, these polymers are not as resistant to fracture compared to polymers that only have acrylic acid in one network. The presence of entanglements in the resulting IPNs and a crosslinked exchangeable anhydride-acrylic acid network enhances their resistance to fracture. In the transient state, anhydride-acrylic acids act as sacrificial bonds in polymer with acrylic acid only in its first network while weakly crosslinked second (permanent) network transfer its load to the more highly crosslinked (transient) second network in the polymer which has acrylic acid in both network (first and second). This is similar to the scenario in traditional double network hydrogels, which also have remarkable toughness.<sup>47</sup> However, because of the possibility of refueling through subsequent addition of EDC, these materials could continue to perform well even after an initial challenge, since anhydrides can be reformed by refueling, as demonstrated in Figure 4.

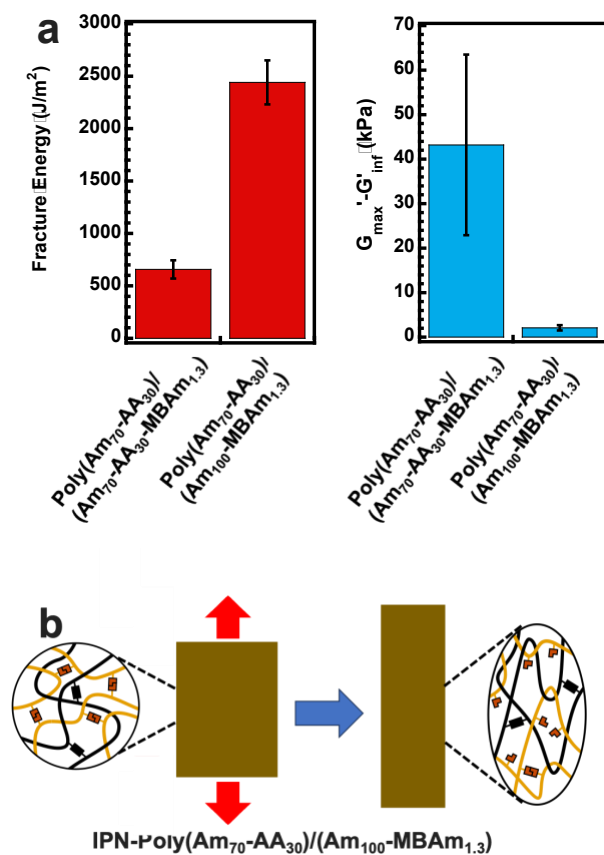


Figure 2: a) Variation of fracture energy and  $G'_{\max}$  polymer architecture. (b) Overview of the polymers during stretching

## Conclusion

Carbodiimides can generate transient IPNs from carboxylic-acid-functionalized polymer networks with exceptional fracture energies, resistance of the material to compression, and enhanced ability deformation. By carefully selecting the network architecture, the mechanical properties of hydrogels, such as peak storage modulus and fracture energy, can be tailored. Surprisingly, materials with relatively modest increases in overall elastic modulus upon fueling demonstrate some of the best fracture energies and tolerance to high compression. These materials transition to an IPN architecture in the activated state, enabling effective energy dissipation. This approach has opened up new possibilities, including the exploration of kirigami-like patterns within hydrogels. This highlights the importance of considering the structural design of hydrogels in order to achieve desired characteristics and performance.

## ASSOCIATED CONTENT

### Supporting Information

The Supporting Information is available free of charge on the ACS Publications website.

Experimental details and supplemental data (PDF)

## AUTHOR INFORMATION

Corresponding Author

\* CSH ([scott.hartley@miamiOH.edu](mailto:scott.hartley@miamiOH.edu))

\* DK ([d.konkolewicz@miamiOH.edu](mailto:d.konkolewicz@miamiOH.edu))

## Author Contributions

C.W.H.R. was involved in lead synthesis and characterization, writing, data visualization. C.T. was involved in characterization, synthesis and kirigami patterning. J.L.S. was involved in mechanical testing. W.H.K. was involved in characterization and synthesis (during REU). C.S.H. was involved in conceptualization, analysis, writing, data visualization. D.K. was involved in conceptualization, analysis, writing, data visualization.

## Funding Sources

This work was supported by United States Department of Energy, Office of Science, Basic Energy Sciences, under Award No. DE-SC0018645 for network synthesis and characterization. 400 MHz NMR instrumentation at Miami University is supported through funding from the National Science Foundation under Award No. CHE-1919850.

## ACKNOWLEDGMENT

The authors thank Miami University for supporting the Instrumentation Laboratory.

## References

- (1) Kariyawasam, L. S.; Hossain, M. M.; Hartley, C. S. The Transient Covalent Bond in Abiotic Nonequilibrium Systems. *Angew. Chem., Int. Ed.* **2021**, *60* (23), 12648–12658.
- (2) Chen, X.; Würbser, M. A.; Boekhoven, J. Chemically Fueled Supramolecular Materials. *Acc. Mater. Res.* **2023**, *4* (5), 416–426.
- (3) Davies, R. E. A Molecular Theory of Muscle Contraction: Calcium-Dependent Contractions with Hydrogen Bond Formation plus ATP-Dependent Extensions of Part of the Myosin-Actin Cross-Bridges. *Nature* **1963**, *199* (4898), 1068–1074.
- (4) Cain, D. F.; Infante, A. A.; Davies, R. E. Chemistry of Muscle Contraction: Adenosine Triphosphate and Phosphorylcreatine as Energy Supplies for Single Contractions of Working Muscle. *Nature* **1962**, *196* (4851), 214–217.
- (5) Rajawasam, C. W. H.; Tran, C.; Weeks, M.; McCoy, K. S.; Ross-Shannon, R.; Dodo, O. J.; Sparks, J. L.; Hartley, C. S.; Konkolewicz, D. Chemically Fueled Reinforcement of Polymer Hydrogels. *J. Am. Chem. Soc.* **2023**, *145* (9), 5553–5560.
- (6) Dodo, O. J.; Petit, L.; Rajawasam, C. W. H.; Hartley, C. S.; Konkolewicz, D. Tailoring Lifetimes and Properties of Carbodiimide-Fueled Covalently Cross-Linked Polymer Networks. *Macromolecules* **2021**, *54* (21), 9860–9867.
- (7) Bai, S.; Niu, X.; Wang, H.; Wei, L.; Liu, L.; Liu, X.; Eelkema, R.; Guo, X.; van Esch, J. H.; Wang, Y. Chemical Reaction Powered Transient Polymer Hydrogels for Controlled Formation and Free Release of Pharmaceutical Crystals. *Chem. Eng. J.* **2021**, *414*, 128877.
- (8) Wang, Z.; Xiao, J.; Zhao, T.; Zhang, C.; Wang, L.; He, N.; Kong, Q.; Wang, X. Transient Regulation of Gel Properties by Chemical Reaction Networks. *Chem. Commun.* **2023**.
- (9) Xu, H.; Bai, S.; Gu, G.; Gao, Y.; Sun, X.; Guo, X.; Xuan, F.; Wang, Y. Bioinspired Self-Resetable Hydrogel Actuators Powered by a Chemical Fuel. *ACS Appl. Mater. Interfaces* **2022**, *14* (38), 43825–43832.

- (10) Heckel, J.; Batti, F.; Mathers, R. T.; Walther, A. Spinodal Decomposition of Chemically Fueled Polymer Solutions. *Soft Matter* **2021**, *17* (21), 5401–5409.
- (11) Ni, C.; Chen, D.; Zhang, Y.; Xie, T.; Zhao, Q. Autonomous Shapeshifting Hydrogels via Temporal Programming of Photoswitchable Dynamic Network. *Chem. Mater.* **2021**, *33* (6), 2046–2053.
- (12) Lu, D.; Zhu, M.; Wu, S.; Lian, Q.; Wang, W.; Adlam, D.; Hoyland, J. A.; Saunders, B. R. Programmed Multiresponsive Hydrogel Assemblies with Light-Tunable Mechanical Properties, Actuation, and Fluorescence. *Adv. Funct. Mater.* **2020**, *30* (11), 1909359.
- (13) Zheng, W. J.; An, N.; Yang, J. H.; Zhou, J.; Chen, Y. M. Tough Al-Alginate/Poly (N-Isopropylacrylamide) Hydrogel with Tunable LCST for Soft Robotics. *ACS Appl. Mater. Interfaces* **2015**, *7* (3), 1758–1764.
- (14) Wojciechowski, J. P.; Martin, A. D.; Thordarson, P. Kinetically Controlled Lifetimes in Redox-Responsive Transient Supramolecular Hydrogels. *J. Am. Chem. Soc.* **2018**, *140* (8), 2869–2874.
- (15) Yesilyurt, V.; Webber, M. J.; Appel, E. A.; Godwin, C.; Langer, R.; Anderson, D. G. Injectable Self-healing Glucose-responsive Hydrogels with PH-regulated Mechanical Properties. *Adv. Mater.* **2016**, *28* (1), 86–91.
- (16) Vedadghavami, A.; Minooei, F.; Mohammadi, M. H.; Khetani, S.; Kolahchi, A. R.; Mashayekhan, S.; Sanati-Nezhad, A. Manufacturing of Hydrogel Biomaterials with Controlled Mechanical Properties for Tissue Engineering Applications. *Acta Biomater.* **2017**, *62*, 42–63.
- (17) Wei, M.; Gao, Y.; Li, X.; Serpe, M. J. Stimuli-Responsive Polymers and Their Applications. *Polym. Chem.* **2017**, *8* (1), 127–143.
- (18) Fu, X.; Hosta-Rigau, L.; Chandrawati, R.; Cui, J. Multi-Stimuli-Responsive Polymer Particles, Films, and Hydrogels for Drug Delivery. *Chem* **2018**, *4* (9), 2084–2107.
- (19) Zhang, D.; Ren, B.; Zhang, Y.; Xu, L.; Huang, Q.; He, Y.; Li, X.; Wu, J.; Yang, J.; Chen, Q. From Design to Applications of Stimuli-Responsive Hydrogel Strain Sensors. *J. Mater. Chem. B* **2020**, *8* (16), 3171–3191.
- (20) Hu, L.; Zhang, Q.; Li, X.; Serpe, M. J. Stimuli-Responsive Polymers for Sensing and Actuation. *Mater. Horiz.* **2019**, *6* (9), 1774–1793.
- (21) Chen, Z.; Liu, J.; Chen, Y.; Zheng, X.; Liu, H.; Li, H. Multiple-Stimuli-Responsive and Cellulose Conductive Ionic Hydrogel for Smart Wearable Devices and Thermal Actuators. *ACS Appl. Mater. Interfaces* **2020**, *13* (1), 1353–1366.
- (22) Deng, Z.; Guo, Y.; Zhao, X.; Ma, P. X.; Guo, B. Multifunctional Stimuli-Responsive Hydrogels with Self-Healing, High Conductivity, and Rapid Recovery through Host–Guest Interactions. *Chem. Mater.* **2018**, *30* (5), 1729–1742.
- (23) Boekhoven, J.; Hendriksen, W. E.; Koper, G. J. M.; Eelkema, R.; van Esch, J. H. Transient Assembly of Active Materials Fueled by a Chemical Reaction. *Science (1979)* **2015**, *349* (6252), 1075–1079.
- (24) Klemm, B.; Lewis, R. W.; Piergentili, I.; Eelkema, R. Temporally Programmed Polymer–Solvent Interactions Using a Chemical Reaction Network. *Nat. Commun.* **2022**, *13* (1), 6242.
- (25) Zhang, Y.; Li, P.; Zhang, K.; Wang, X. Temporary Actuation of Bilayer Polymer Hydrogels Mediated by the Enzymatic Reaction. *Langmuir* **2022**, *38* (49), 15433–15441.
- (26) Zhang, C.; Lu, H.; Wang, X. Transient Polymer Hydrogels Based on Dynamic Covalent Borate Ester Bonds. *Chin. J. Chem.* **2022**, *40* (23), 2794–2800.
- (27) Kariyawasam, L. S.; Hartley, C. S. Dissipative Assembly of Aqueous Carboxylic Acid Anhydrides Fueled by Carbodiimides. *J. Am. Chem. Soc.* **2017**, *139* (34), 11949–11955.

- (28) Tena-Solsona, M.; Rieß, B.; Grötsch, R. K.; Löhner, F. C.; Wanzke, C.; Käs Dorf, B.; Bausch, A. R.; Müller-Buschbaum, P.; Lieleg, O.; Boekhoven, J. Non-Equilibrium Dissipative Supramolecular Materials with a Tunable Lifetime. *Nat. Commun.* **2017**, *8* (1), 15895.
- (29) Heckel, J.; Loescher, S.; Mathers, R. T.; Walther, A. Chemically Fueled Volume Phase Transition of Polyacid Microgels. *Angew. Chem.* **2021**, *133* (13), 7193–7201.
- (30) Watuthantrige, N. D. A.; Chakma, P.; Konkolewicz, D. Designing Dynamic Materials from Dynamic Bonds to Macromolecular Architecture. *Trends Chem.* **2021**, *3* (3), 231–247.
- (31) Zoratto, N.; Matricardi, P. Semi-IPNs and IPN-Based Hydrogels. *Polym. Gels* **2018**, 91–124.
- (32) Dhand, A. P.; Galarraga, J. H.; Burdick, J. A. Enhancing Biopolymer Hydrogel Functionality through Interpenetrating Networks. *Trends Biotechnol.* **2021**, *39* (5), 519–538.
- (33) Qiu, X.; Winnik, F. M. Facile and Efficient One-Pot Transformation of RAFT Polymer End Groups via a Mild Aminolysis/Michael Addition Sequence. *Macromol. Rapid Commun.* **2006**, *27* (19), 1648–1653.
- (34) Zhang, B.; Jayalath, I. M.; Ke, J.; Sparks, J. L.; Hartley, C. S.; Konkolewicz, D. Chemically Fueled Covalent Crosslinking of Polymer Materials. *Chem. Commun.* **2019**, *55* (14), 2086–2089.
- (35) Zhang, B.; Ke, J.; Vakil, J. R.; Cummings, S. C.; Digby, Z. A.; Sparks, J. L.; Ye, Z.; Zanjani, M. B.; Konkolewicz, D. Dual-Dynamic Interpenetrated Networks Tuned through Macromolecular Architecture. *Polym. Chem.* **2019**, *10* (46), 6290–6304.
- (36) Panteli, P. A.; Patrickios, C. S. Multiply Interpenetrating Polymer Networks: Preparation, Mechanical Properties, and Applications. *Gels* **2019**, *5* (3), 36.
- (37) Sun, J.-Y.; Zhao, X.; Illeperuma, W. R. K.; Chaudhuri, O.; Oh, K. H.; Mooney, D. J.; Vlassak, J. J.; Suo, Z. Highly Stretchable and Tough Hydrogels. *Nature* **2012**, *489* (7414), 133–136.
- (38) Cummings, S. C.; Dodo, O. J.; Hull, A. C.; Zhang, B.; Myers, C. P.; Sparks, J. L.; Konkolewicz, D. Quantity or Quality: Are Self-Healing Polymers and Elastomers Always Tougher with More Hydrogen Bonds? *ACS Appl. Polym. Mater.* **2020**, *2* (3), 1108–1113.
- (39) Zhao, X.; Chen, X.; Yuk, H.; Lin, S.; Liu, X.; Parada, G. Soft Materials by Design: Unconventional Polymer Networks Give Extreme Properties. *Chem Rev* **2021**, *121* (8), 4309–4372.
- (40) Wanasinghe, S. V.; Schreiber, E. M.; Thompson, A. M.; Sparks, J. L.; Konkolewicz, D. Dynamic Covalent Chemistry for Architecture Changing Interpenetrated and Single Networks. *Polym. Chem.* **2021**, *12* (13), 1975–1982.
- (41) Bunton, C. A.; Fuller, N. A.; Perry, S. G.; Shiner, V. J. The Pyridine Catalysed Hydrolysis of Carboxylic Anhydrides. *Tetrahedron Lett.* **1961**, *2* (14), 458–460.
- (42) Gong, J. P. Why Are Double Network Hydrogels so Tough? *Soft Matter* **2010**, *6* (12), 2583–2590.
- (43) Ji, D.; Nguyen, T. L.; Kim, J. Bioinspired Structural Composite Hydrogels with a Combination of High Strength, Stiffness, and Toughness. *Adv. Funct. Mater.* **2021**, *31* (28), 2101095.
- (44) Freedman, B. R.; Uzun, O.; Luna, N. M. M.; Rock, A.; Clifford, C.; Stoler, E.; Östlund-Sholars, G.; Johnson, C.; Mooney, D. J. Degradable and Removable Tough Adhesive Hydrogels. *Adv. Mater.* **2021**, *33* (17), 2008553.
- (45) Bunton, C. A.; Fuller, N. A.; Perry, S. G.; Shiner, V. J. The Pyridine Catalysed Hydrolysis of Carboxylic Anhydrides. *Tetrahedron Lett* **1961**, *2* (14), 458–460.

- (46) Li, X.; Wang, L.; Li, Y.; Xu, S. Reprocessable, Self-Healing, Thermadappt Shape Memory Polycaprolactone via Robust Ester–Ester Interchanges Toward Kirigami-Tailored 4D Medical Devices. *ACS Appl. Polym. Mater.* **2023**, *5* (2), 1585–1595.
- (47) Gong, J. P.; Katsuyama, Y.; Kurokawa, T.; Osada, Y. Double-network Hydrogels with Extremely High Mechanical Strength. *Adv. Mater.* **2003**, *15* (14), 1155–1158.